Effects of Molecular Weight on the Miscibility and Properties of Polyurethane/Benzyl Starch Semi-Interpenetrating Polymer Networks

Xiaodong Cao and Lina Zhang*

Department of Chemistry, Wuhan University, Wuhan 430072, China

Received July 31, 2004; Revised Manuscript Received November 11, 2004

We successfully prepared a series of semi-interpenetrating polymer networks (semi-IPNs) from castor oil-based polyurethane (PU) and 20 wt % benzyl starch (BS) with different weight-average molecular weights (M_w), coded as the PU/BS films. The M_w values of a series of BSs were determined by size-exclusion chromatography combined with laser light scattering. The effects of the BS M_w on the miscibility and properties of the resulting PU/BS films were investigated using reflection Fourier transform infrared spectroscopy, differential scanning calorimetry, dynamic mechanical thermal analysis, scanning electron microscopy, optical microscopy, ultraviolet−visible spectroscopy, and tensile testing. The results revealed that the PU/BS films possessed much higher optical transmittance and tensile strength than the pure PU film. Interestingly, with a decrease of the BS M_w from 1.69×10^7 to 5.70×10^5, the optical transmittance, tensile strength, and elongation at break of the PU/BS films increased from 82% to 89%, from 11.7 to 15.7 MPa, and from 121% to 180%, respectively. Therefore, the M_w of BS plays an important role in the improvement of the miscibility and properties of the semi-IPN materials. On the basis of the analysis of the miscibility and the morphology of the PU/BS films, the interaction between the PU and the BS with relatively low M_w was stronger than that with high M_w.

Introduction

There is a growing urgency to develop novel bio-based products and innovative technologies that can lessen widespread dependence on fossil fuel.[1−6] Starch is a potential candidate for the fossil fuel, because it is renewable, abundant, and cheap. However, starch is mostly water-soluble, difficult to process, and brittle when used without plasticizers. Furthermore, its mechanical properties are very sensitive to moisture content, which is difficult to control.[7] Thus, the various physical or chemical modifications of starch have been considered, including blending,[8−10] chemical derivatization,[11] and graft copolymerization.[12,13] The starch derivatives with high hydrophobicity have good compatibility with synthetic plastics,[14] and a composite material from starch propionate and polyester polyurethane exhibits better interfacial adhesion and miscibility than normal starch-blended polyurethane.[15] Recently, the effects of the weight-average molecular weight (M_w) of any component on the structure, miscibility, and properties of the composite materials have attracted much attention.[16−25] The following have been reported: the effects of polyamide molecular weight on morphology, Izod impact toughness, and ductile−brittle transition temperature in the nylon 6 blends with maleated elastomers;[16−18] better compatibility of the lower molecular weight of atactic polystyrene-*b*-poly(ethylene-*co*-butylene)-*b*-atactic polystyrene (SEBS) in the syndiotactic polystyrene (sPS)/ethylenepropylene (EPR) blends than the higher molecular weight SEBS;[21] molecular weight effect on the thermal properties and crystal structure of syndiotactic polystyrene/atactic polystyrene blends.[22] However, the effects of the M_w of natural polymers on the structure and physical properties of the composite or blends have been scarcely published.

An interpenetrating polymer network (IPN) is defined as a combination of two or more polymeric networks, at least one of which is cross-linked in the presence of the other.[26] The naturally occurring polymers can be interpenetrated into the polyurethane (PU) networks to form a semi-IPN, which provides a new technology for modification of starch. In our laboratory, semi-IPN materials derived from castor oil-based PU and derivatives of natural polymers, such as nitrocellulose,[27] nitrokonjac glucomannan,[28] and benzyl konjac glucomannan (B-KGM),[29,30] have been studied, and the observations point out that the incorporation of the natural polymers into PU plays an important role in accelerating curing and enhancing biodegradability. Moreover, the PU/natural polymer materials can be degraded by microorganisms in soil, along with the degraded production of CO_2, H_2O, and aromatic ethers.[31] Furthermore, the composites containing benzyl groups have been used as biodegradable biomaterials.[32,33] In previous work, we have prepared a series of semi-IPNs from benzyl starch (BS) and PU, which has good or certain miscibility in the range of BS content from 5 to 70 wt %.[34] In the present work, BSs with different M_w values were synthesized, and then the semi-IPN films from PU and BS were prepared. The effects of BS M_w on the miscibility and various properties were investigated, and

* To whom correspondence should be addressed. Phone: +86-27-87219274. Fax: +86-27-68756661. E-mail: lnzhang@public.wh.hb.cn.

10.1021/bm0495598 CCC: $30.25
Published on Web 01/06/2005

hopefully our work may contribute meaningful information to the understanding of the correlation of the secondary structure to the properties of materials.

Experimental Section

Materials. 4,4′-Diphenylmethane diisocyanate (MDI) was purchased from Aldrich Co. Other reagents and solvents were obtained from commercial sources in China. The cornstarch was supplied from Wuhan Starch Co. (Wuhan, China), which consists of about 75% amylopectin and 25% amylose. The castor oil (a chemical reagent with a 4.49 wt % content of hydroxyl groups and hydroxyl value of 163, AOCS) was dried at 110 °C under 20 mmHg for 2 h. *N*,*N*-Dimethylformamide (DMF) was dried over molecular sieves (4 Å) for 1 week before use. The other reagents were used without further purification.

Preparation of BS Fractions. A 20 g sample of starch was introduced into 200 mL of 20 wt % sulfuric acid aqueous solution at 25 °C, and the resulting solution was stirred for the desired time. The resulting solution was filtered and washed with distilled water to pH 7. Then the product was dispersed in 200 mL of water and introduced into a three-necked flask equipped with a mechanical stirrer, a dropping funnel, and a condenser. The flask was placed in an oil bath at 40 °C and stirred vigorously, while 100 g of 35 wt % sodium hydroxide aqueous solution was added dropwise. The resulting alkali−starch slurry was stirred at 40 °C for 30 min before 50 g of benzyl chloride was added dropwise. The benzylation reaction was performed at about 100 °C for 1 h to obtain a white precipitate. The precipitate was washed with acetone and water alternately more than five times and then vacuum-dried at room temperature to obtain a white powder of benzyl starch. By adjusting the degradation time of starch in sulfuric acid aqueous solution for 0, 2, 5, 8, 12, and 24 h, a series of the BS products with different M_w values were synthesized and coded as BS0, BS2, BS5, BS8, BS12, and BS24, respectively.

Preparation of PU/BS. A four-necked flask was fitted with a nitrogen inlet tube, a mechanical stirrer, a thermometer, and a pressure-equalizing dropping funnel. A 50 g sample of MDI was poured into flask and then heated for melting at 40 °C. To the flask under a nitrogen atmosphere was added dropwise 69 g of castor oil. The dropping was completed within 50 min, and then the stirring was continued for 2 h to get the PU prepolymer.

PU prepolymer, 20 wt % BS, and 1,4-butanediol as the chain extender (the amount being adjusted to give total [NCO]/[OH] = 1) were dissolved in DMF at room temperature. The resulting mixture was given a solid content of about 10 wt %, and then it was cast onto a glass plate and cured at 60 °C for 12 h to obtain a transparent PU/BS semi-IPN film. The resulting PU/BS films with thickness of about 200 μm were peeled off, and were coded as PU/BS0, PU/BS2, PU/BS5, PU/BS8, PU/BS12, and PU/BS24, depending on the BS M_w. The PU film was prepared identically, but cured for 24 h, which was much longer than that of the PU/BS films. The resulting films were vacuumed-dried at room temperature for 3 days and kept in a desiccator with P_2O_5 as the desiccant for more than 1 week before characterization.

Characterization. Size-exclusion chromatography combined with laser light scattering (SEC−LLS) is an absolute method of M_w measurement. The M_w of BS was determined with multiangle laser light scattering (DAWN-DSP, Wyatt Technology Co., Santa Barbara, CA) combined with a pump P100 (Thermo Separation Products) equipped with a TSK-GEL G5000 HHR column (7.8 mm × 300 mm) and a differential refractive index detector (RI-150) in DMF at 25 °C. The refractive index increment (d*n*/d*c*) of BS in DMF was measured with a double-beam differential refractometer (DRM-1020, Otsuka Electronics Co., Japan) at 633 nm and 25 °C to be 0.162 mL g^{-1}. Astra software was utilized for data acquisition and analysis. The degree of substitution (DS) of the BS was calculated from elemental data obtained by using an elemental analyzer (CHN-O-RAPID, Heraeus Co., Germany).

Attenuated total reflection Fourier transform infrared (ATR-FTIR) spectroscopy of the films was performed on an FTIR spectrometer (1600, Perkin-Elmer Co.). The samples were taken at random from flat films, and the data were collected over 32 scans with a resolution of 4 cm^{-1} at room temperature.

To observe clearly the dispersion of BS, the PU/BS films enclosed in a nylon mesh were immersed in DMF accompanied by mild stirring for 1 week at room temperature, and DMF was refreshed five times; thus, the BS with weak interaction with the PU was dissolved mainly in DMF and removed during the extraction process. Scanning electron microscopy (SEM) images were taken on an SEM microscope (Hitachi S-570, Japan). The extracted films were frozen in liquid nitrogen and snapped immediately, and the cross-sections of the films were coated with gold for SEM observation. The optical micrographs with phase contrast of the surface of the extracted films were obtained with a microscope (Axiovert 200M, Zeiss, Germany) and a high-resolution digital camera (AxioCam, up to 3900 × 3090 pixels, Zeiss).

Differential scanning calorimetry (DSC) measurement of the films was carried out on a DSC apparatus (200 PC, Netzsch Co., Germany) under a nitrogen atmosphere at a heating rate of 20 °C min^{-1} from −50 to +200 °C. Prior to the test, samples of about 10 ± 1 mg were heated from room temperature to 100 °C, and then maintained at that temperature for 2 min to remove moisture and other volatile components in the films. The resulting samples were quenched to −50 °C to measure the DSC curves. In addition, the BS was measured with the process mentioned above, but the temperature range changed from 40 to 180 °C.

Dynamic mechanical thermal analysis (DMTA) was carried out on a dynamic mechanical thermal analyzer (DMTA-V, Rheometric Scientific Co.) in rectangular tension mode. The temperature program was run from −50 to +200 °C using a heating ramp of 5 °C min^{-1} at a fixed frequency of 1 Hz. Specimens with a typical size of 10 mm × 10 mm (length × width) were used.

The densities (ρ) of the samples were measured at 25 °C by determining the weight of a volume-calibrated psychomotor filled with a mixture of NaCl aqueous solution and distilled water, in which the samples achieved the flotation

Table 1. Experimental Results of M_w and DS for BS

	sample					
	BS0	BS2	BS5	BS8	BS12	BS24
$M_w \times 10^{-6}$	16.91	7.59	3.42	1.84	1.08	0.57

level. The density of the liquid mixture equals the density of the samples. Three parallel measurements were carried out for each sample. The percent optical transmittance of the films with a thickness of about 200 μm was measured by using an ultraviolet−visible spectrophotometer (UV-160A, Shimadzu, Japan) at 500 and 800 nm, respectively. The moisture contents of the PU/BS films were achieved by conditioning the samples at room temperature in desiccators at controlled humidity containing saturated salt aqueous solutions. Three relative humidities (RHs) at 20−25 °C were used, namely, 35%, 75%, and 98%. The saturated salt solutions were $CaCl_2 \cdot 6H_2O$, NaCl, and $CuSO_4 \cdot 5H_2O$, respectively. The conditioning was achieved for at least 2 weeks to ensure the equilibration of the water content in the films with that of the atmosphere (stabilization of the sample weight).[7] The tensile strength and elongation at break of the films were measured on a universal testing machine (CMT 6503, Shenzhen SANS Test Machine Co. Ltd., China) at room temperature with a tensile rate of 50 mm min^{-1} according to ISO6239-1986 (E), and an average value of at least five replicates for each sample was taken.

Results and Discussion

Effects of BS M_w on Structure and Morphology. The experimental results of M_w for the six BS fractions are summarized in Table 1. The data indicated that the M_w of the resulting BS decreases from 1.69×10^7 to 5.70×10^5, with an increase of the degradation time of the native starch in 20 wt % sulfuric acid aqueous solution from 0 to 24 h. In addition, the DS values of the six samples approach a uniform value of about 0.94 ± 0.06. FTIR spectroscopy can be used to investigate the interaction of hard and soft segments of PU and obtain information on hydrogen bonding in the samples. In a pure urethane hard domain, hydrogen bonding results from the hydrogen atoms of NH groups serving as proton donors and the C═O groups acting as proton acceptors. When the urethane hard segment and the castor oil soft segment are mixed at the molecular level, the C═O groups and the oxygens in the castor oil backbone also can act as proton acceptors in the formation of hydrogen bonds with the NH groups of the hard segment urethane groups. ATR-FTIR spectra of the urethane carbonyl region for the PU and PU/BS films are shown in Figure 1. There are two major bands centered at approximately 1727 and 1708 cm^{-1} in all spectra, which are assigned to free C═O groups and hydrogen-bonded C═O groups in ordered domains of PU, respectively.[35] The intensity of the hydrogen-bonded C═O groups in ordered domains of the PU/BS films is lower than that of the PU films, and the relative intensity of the free C═O band increases with a decrease of the BS M_w from 1.69×10^7 to 5.70×10^5. This illustrates that the introduction of BS can disturb the hydrogen bonds in PU itself, leading to more free C═O groups of PU in the PU/BS films with lower M_w BS than in those with higher M_w BS. Moreover, the absorption band of hydrogen-bonded C═O groups splits into two peaks for the PU/BS films having BS with M_w lower than 1.84×10^6; namely, a shoulder peak appears at about 1717 cm^{-1}, which is assigned to hydrogen-bonded C═O groups in disordered domains, suggesting a relatively strong interaction between BS and PU. This can be explained by the fact that BS molecules with lower M_w can more easily penetrate into the PU networks and interact with them than those with higher M_w, resulting in the inhibition of the hydrogen bonding in PU itself.

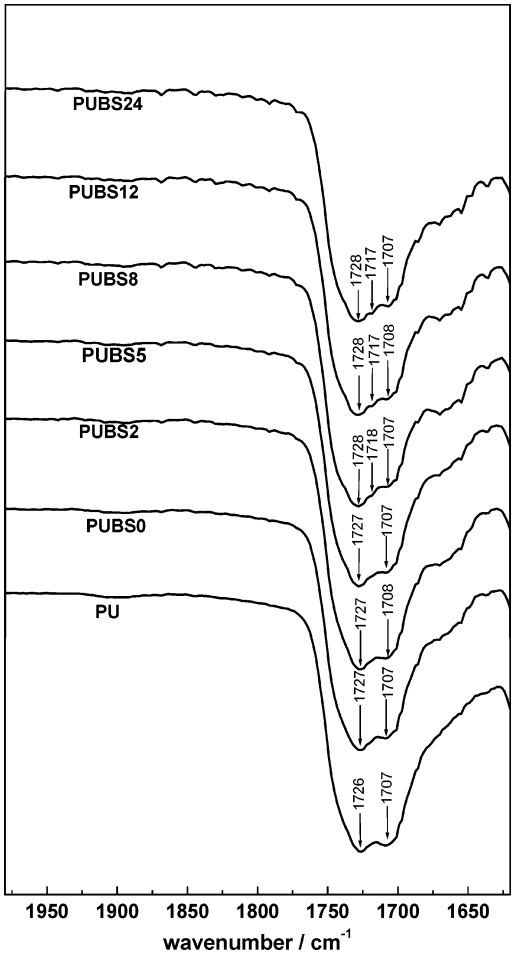

Figure 1. ATR-FTIR spectra of the PU/BS and PU films.

The SEM images of cross-sections of the PU/BS films extracted with DMF are shown in Figure 2. The dark domain is the void, where the BS molecules have been removed during the extraction process as a result of a good solubility of BS in DMF. Obviously, the cross-linked PU has formed a continuous phase, and the BS is dispersed in it. The dark domains decrease with a decrease of BS M_w; namely, BS exists as small-sized particles in the PU/BS12 and PU/BS24 films, confirming that the BS with low M_w more easily penetrates into PU networks to be dispersed in them as a result of the stronger interaction with PU molecules than that with high M_w. Therefore, the PU/BS films with low-M_w BS have better miscibility and more uniform morphology. Figure 3 shows optical micrographs with phase contrast of the surface of the PU/BS films. It reveals that the PU/BS film with high-M_w BS has a relatively coarse surface, indicating that the high-M_w BS is dispersed in the PU matrix with a

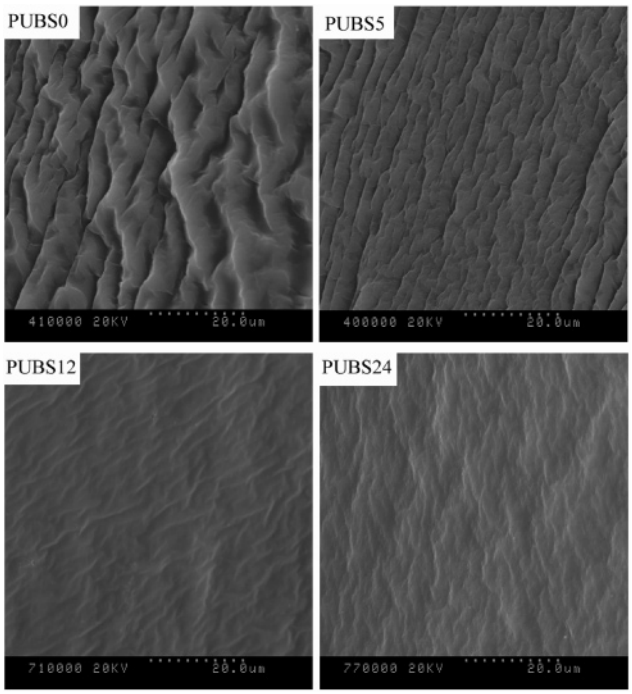

Figure 2. SEM images of the cross-sections of the PU/BS films.

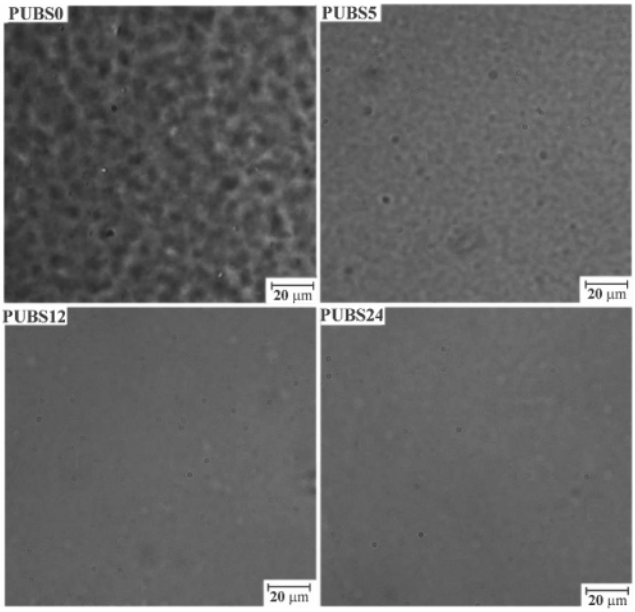

Figure 3. Phase contrast micrographs of the surface of the PU/BS films.

relatively large phase domain size. Meanwhile, the PU/BS12 and PU/BS24 films exhibit a smooth and compact surface, suggesting that better miscibility exists between the PU and the low-M_w BS. This result is in good agreement with that of SEM. The densities of PU/BS films as a function of the BS M_w are shown in Figure 4. It is worth noting that the densities of the PU/BS films are higher than that of the PU film, and approach a constant regardless of the BS M_w, further confirming that a relatively strong interaction occurs between PU and BS in the PU/BS films.

Effects of BS M_w on Miscibility. Usually, DSC and DMTA can be used extensively to study the miscibility of different polymer blends.[36] The DSC thermograms of the BS0, PU, and PU/BS films are shown in Figure 5, and the

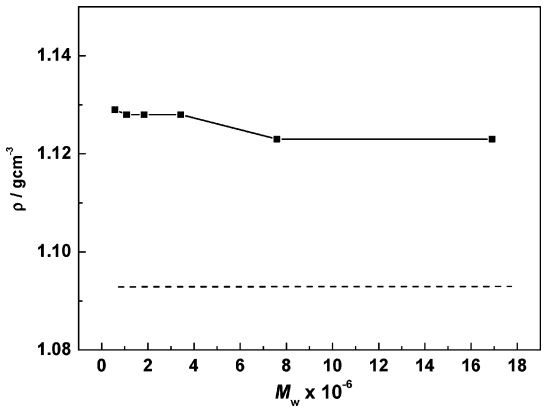

Figure 4. Dependence of density (ρ) on the BS M_w of the PU/BS films. The dashed line represents the ρ of the PU film.

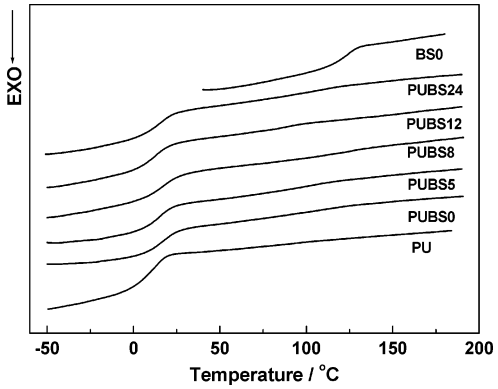

Figure 5. DSC thermograms of the BS0, PU/BS, and PU films.

Table 2. Results from DSC and DMTA of BS0, PU, and PU/BS Films

			α_1 transition		α_2 transition	
sample	T_g(mid)/ °C	ΔC_p/ g^{-1} K^{-1}	$T_{\alpha1}$/ °C	tan δ	$T_{\alpha2}$/ °C	tan δ
PU	17.3	0.464	24.6	1.08		
PU/BS0	16.1	0.334	24.4	0.66	144.7	0.42
PU/BS5	14.7	0.336	25.0	0.79	155.6	0.34
PU/BS8	14.6	0.316	*a*	*a*	*a*	*a*
PU/BS12	13.8	0.350	28.6	0.91	156.6	0.26
PU/BS24	13.9	0.305	30.1	0.87	159.2	0.33
BS0	126.5	0.228	*a*	*a*	*a*	*a*

[a] Not measured.

corresponding data are summarized in Table 2. In the DSC curves, the midpoint of the step of the thermogram is taken as the glass transition temperature (T_g). Interestingly, there is only one glass transition region (T_g) to be attributed to PU soft segments in the thermograms of the PU/BS films, whereas T_g attributed to 20 wt % BS is hardly observed in this case, indicating a certain degree of phase mixing between the PU and the BS. Moreover, the introduction of BS into PU results in a slight reduction of T_g of the PU/BS films, compared with the PU film. This can be explained by a plasticization effect,[37] perhaps more importantly, by incompetently formed PU networks containing loose chain ends as a result of the dilution effect of the incorporation of BS into the PU network.[38−40] It is noted that the soft segments dissolved in hard segments or other microphases are not expected to contribute to the heating capacity (ΔC_p), since their mobility is restricted.[41] The values of ΔC_p of the PU/

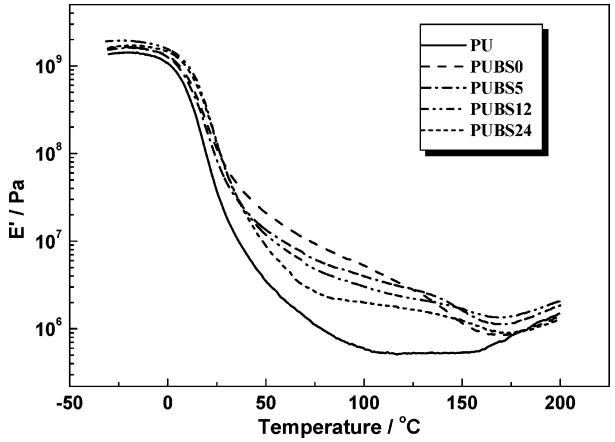

Figure 6. Temperature dependence of the storage modulus (E') for the PU and PU/BS films.

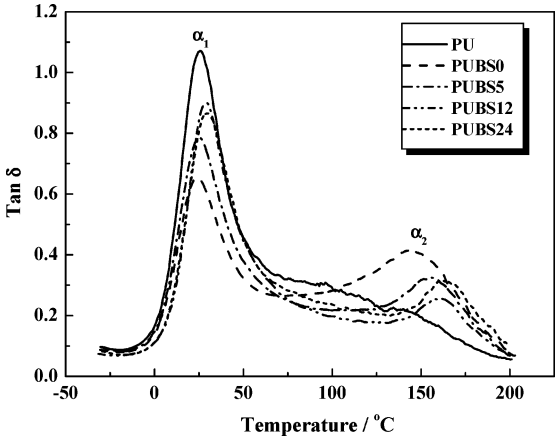

Figure 7. Temperature dependence of the mechanical loss factor (tan δ) for the PU and PU/BS films.

BS films are lower than that of the PU component, suggesting a decrease of free soft segments in PU as a result of the strong interfacial adhesion between the BS and the PU.

The temperature dependence of the storage modulus (E') for the PU and PU/BS films is shown in Figure 6. The E' curves of all PU/BS films display two distinctive drops in stiffness at low and high temperature, assigned to the glass transition of the PU soft segments and the BS, respectively. The DMTA curve can reflect the glass transition of the BS component, because the sensitivity of DMTA is much higher than that of DSC.[42] The loss factor (tan δ) of the PU and PU/BS films as a function of temperature is plotted in Figure 7, and the peak positions and the height of tan δ are summarized in Table 2. The pure BS is too brittle, so we cannot obtain the corresponding data of its film for DMTA. The two tan δ peaks of PU/BS films, corresponding to the glass transition temperature, are assigned to the soft segments of PU ($T_{\alpha 1}$) at about 25 °C and to the BS ($T_{\alpha 2}$) at about 155 °C, respectively. The sharpness and height of the damping peaks can give information about the degree of order and the freedom of motion of molecules in the soft domains, and the T_α shift is related to the degree of the interaction between the components.[43] The $T_{\alpha 1}$ of the PU/BS films increases with a decrease of BS M_w, suggesting the stronger interaction between the BS with lower M_w and PU than that between the BS with higher M_w and PU. Therefore, the interaction induces certain miscibility in the composites and prohibits

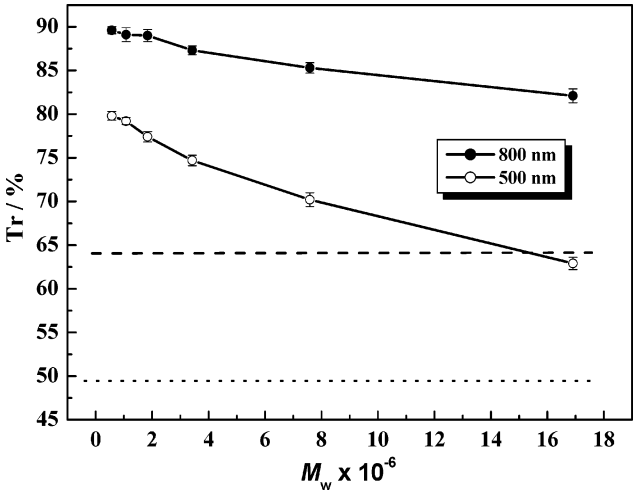

Figure 8. Effect of BS M_w on the optical transmittance (Tr) of the PU/BS films at 500 and 800 nm. Dotted and dashed lines represent the Tr of the PU film at 500 and 800 nm, respectively.

the mobility of the PU macromolecules. Interestingly, the glass transition $T_{\alpha 2}$ shifts to high temperature with a decrease of the BS M_w, suggesting that the motion of BS molecules with low M_w is more difficult than that of BS molecules with high M_w. Usually, macromolecules with low M_w are easier to move. Therefore, this result further proves that PU molecules adhere more tightly to BS with low M_w, leading to the enhancement of the thermal property of the PU/BS films.

The transparency of the films is an auxiliary criterion to judge the miscibility of the composites.[44] Generally, the enhancement of light transmittance (Tr) of the polymer blends may be correlative with the interfacial interactions, amorphous state, phase domain size, and match of the refractive indices of the components. The dependences of Tr at 500 and 800 nm on BS M_w for the PU/BS films are shown in Figure 8. Interestingly, the Tr values of the PU/BS films are higher than that of the pure PU film, suggesting that strong interfacial adhesion exists between the BS and the PU, and the BS particles are dispersed in the PU matrix very proportionally. Moreover, the Tr values of the PU/BS films increase from 62.9% to 79.8% and from 82.1% to 89.6% at 500 and 800 nm, respectively, with a decrease of the BS M_w from 1.69×10^7 to 5.70×10^5, indicating that the BS with lower M_w can more easily penetrate and be homogeneously dispersed in the PU network. Therefore, the reduction of BS M_w can enhance the miscibility between the BS and the PU.

Effect of BS M_w on Properties. The water uptake at equilibrium of the PU/BS films at different relative humidities is plotted in Figure 9. It is observed that the water uptake at equilibrium increases with RH to a maximum of about 3% w/w at 98% RH and maintains an approximate value independent of the change of the BS M_w. This result illustrates that the PU/BS films have good water resistivity, differing significantly from that of the starch with high water sensibility.

The dependence of tensile strength (σ_b), Young's modulus, and elongation at break (ϵ_b) on BS M_w for the PU/BS films is shown in Figures 10 and 11, respectively. The pure BS

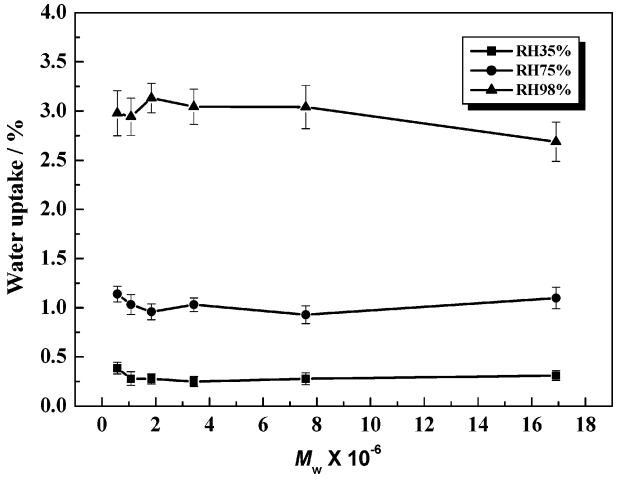

Figure 9. Effect of BS M_w on the water uptake at equilibrium of the PU/BS films at different relative humidities.

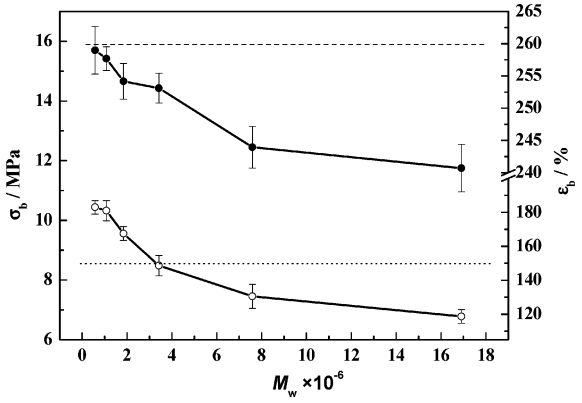

Figure 10. Dependence of tensile strength (σ_b, ●) and elongation at break (ϵ_b, ○) of the PU/BS films on BS M_w. Dotted and dashed lines represent tensile strength and elongation at break for the PU film, respectively.

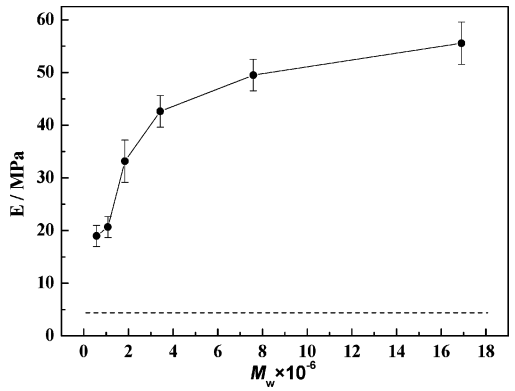

Figure 11. Dependence of the modulus of the PU/BS films on BS M_w. The dashed line represents the modulus for the PU film.

film is too brittle, so its mechanical data of σ_b and ϵ_b cannot be obtained. The great enhancement of σ_b for the PU/BS films compared with the pure PU film indicates that the 20 wt % BS acts as a reinforcement particle. It is worth noting that both σ_b and ϵ_b of the PU/BS films obviously increase with a decrease of the BS M_w from 1.69×10^7 to 5.70×10^5. Moreover, the PU/BS films having BS M_w lower than about 1.0×10^6, namely, the PU/BS12 and PU/BS24 films, possess obviously higher σ_b and ϵ_b. Furthermore, the modulus of the PU/BS films decreases with a decrease of the BS M_w, approaching the nature of an elastomer. Therefore, the relatively low M_w BS plays an important role in the simultaneous enhancement of the tensile strength and the elasticity of the PU/BS films compared with the high-M_w BS. This work provides a significant technological interest for the design of environmentally friendly materials from renewable resources.

Conclusions

The semi-interpenetrating polymer network films were prepared successfully from PU and BS with M_w from 5.70×10^5 to 1.69×10^7 by using solution blending. The experimental results from ATR-FTIR, SEM, and optical microscopy revealed that the BS with lower M_w could more easily penetrate and be homogeneously dispersed in the PU networks to form a uniform and dense morphology as a result of good miscibility. The measurements of DSC, DMTA, optical transmittance, and the tensile test confirmed that the PU/BS films possessed higher thermal stability, optical transmittance, and tensile strength than both PU and BS films, owing to the interaction between molecules of BS and PU. It is worth noting that the mechanical properties, optical transmittance, and thermal stability obviously increased with a decrease of BS M_w from 1.69×10^7 to 5.70×10^5, and reach a plateau when the BS M_w is lower than 1.0×10^6. Therefore, the relatively low BS M_w plays an important role in the improvement of the miscibility between PU and BS as well as the properties of the PU/BS films.

Acknowledgment. This work was supported by major grants of the National Natural Science Foundation of China (59933070), the National Sciences Foundation of China (20474048), and the Laboratory of Cellulose and Lignocellulosic Chemistry of the Chinese Academy of Sciences.

References and Notes

(1) Mathew, A.; Dufresne, A. *Biomacromolecules* **2002**, *3*, 1101−1108.
(2) Nair, K. G.; Dufresne, A. *Biomacromolecules* **2003**, *4*, 657−665.
(3) Mohanty, A. K.; Misra, M.; Drzal, L. T. *J. Polym. Environ.* **2002**, *10*, 19−26.
(4) Li, F.; Larock, R. C. *J. Appl. Polym. Sci.* **2001**, *80*, 658−670.
(5) Li, F.; Hanson, M.; Larock, R. C. *Polymer* **2001**, *42*, 1567−1679.
(6) Lu, Y.; Weng, L.; Zhang, L. *Biomacromolecules* **2004**, *5*, 1046−1051.
(7) Neus Anglès, M.; Dufresne, A. *Macromolecules* **2000**, *33*, 8344−8353.
(8) Mani, R.; Tang, J.; Bhattacharya, M. *Macromol. Rapid Commun.* **1998**, *19*, 283−286.
(9) Neus Anglès, M.; Dufresne, A. *Macromolecules* **2001**, *34*, 2921−2931.
(10) Dufresne, A.; Vignon, M. R. *Macromolecules* **1998**, *31*, 2693−2696.
(11) Sugar, A. D.; Merrill, E. W. *J. Appl. Polym. Sci.* **1995**, *58*, 1647−1656.
(12) Suda, K.; Kanlaya, M.; Manit, S. *Polymer* **2002**, *43*, 3915−3924.
(13) Choi, E. J.; Kim, C. H.; Park, J. K. *Macromolecules* **1999**, *32*, 7402−7408.
(14) Lübecke, P. M.; Köng, W. A. *Carbohydr. Res.* **1989**, *185*, 113−118.
(15) Santayannon, R.; Wootthikanokkhan, J. *Carbohydr. Polym.* **2003**, *51*, 17−24.
(16) Oshinski, A. J.; Keskkula, H.; Paul, D. R. *Polymer* **1996**, *37*, 4891−4907.
(17) Oshinski, A. J.; Keskkula, H.; Paul, D. R. *Polymer* **1996**, *37*, 4809−4918.
(18) Oshinski, A. J.; Keskkula, H.; Paul, D. R. *Polymer* **1996**, *37*, 4819−4928.

(19) Lipson, J. E. G.; Tambasco, M.; Willets, K. A.; Huggins, J. S. *Macromolecules* **2003**, *36*, 2977−2984.
(20) Ahn, J. H.; Zin, W. C. *Macromolecules* **2002**, *35*, 10238−10240.
(21) Hong, B. K.; Jo, W. H. *Polymer* **2000**, *41*, 2069−2079.
(22) Chiu, F. C.; Peng, C. G. *Polymer* **2002**, *43*, 4879−4886.
(23) Yin, Z.; Koulic, C.; Jeon, H. K.; Pagnoulle, C.; Macosko, C. W.; Jérôme, R. *Macromolecules* **2002**, *35*, 8917−8919.
(24) Zhou, P.; Chen, X.; Frisch, H. L.; Zhu, Z.; Rider, J.; Wnek, G. E. *Macromolecules* **1992**, *25*, 7334−7337.
(25) Kayano, Y.; Keskkula, H.; Paul, D. R. *Polymer* **1996**, *37*, 4505−4518.
(26) Erbil, C.; Kazancıoğlu, E.; Uyanık, N. *Eur. Polym. J.* **2004**, *40*, 1145−1154.
(27) Zhang, L.; Zhou, Q. *J. Polym Sci., Part B: Polym. Phys.* **1999**, *37*, 1623−1631.
(28) Gao, S.; Zhang, L. *Macromolecules* **2001**, *34*, 2202−2207.
(29) Lu, Y.; Zhang, L. *Polymer* **2002**, *43*, 3979−3986.
(30) Lu, Y.; Zhang, L. *Polymer* **2003**, *44*, 6689−6696.
(31) Zhang, L.; Zhou, J.; Huang, J.; Gong, P.; Zhou, Q.; Zheng, L.; Du, Y. *Ind. Eng. Chem. Res.* **1998**, *38*, 4284−4289.
(32) Avitabile, T.; Marano, F.; Castiglione, F.; Bucolo, C.; Cro, M.; Ambrosio, L.; Ferrauto, C.; Reibaldi, A. *Biomaterials* **2001**, *22*, 195−200.
(33) Stolnik, S.; Garnett, M. C.; Davies, M. C.; Illum, L.; Bousta, M.; Vert, M.; Davis, S. S. *Colloids Surf., A* **1995**, *97*, 235−245.
(34) Zhang, L.; Cao, X. (Wuhan University). Patent CN 200410012815.8, 2004.
(35) Yen, F. S.; Hong, J. L. *Macromolecules* **1997**, *30*, 7927−7938.
(36) Yu, L.; Christie, G. *Carbohydr. Polym.* **2001**, *46*, 179−184.
(37) Mishra, V.; Du Prez, F.; Sperling, L. H. *J. Polym. Mater. Sci. Eng.* **1995**, *72*, 124.
(38) Zhou, Q.; Zhang, L.; Zhang, M.; Wang, B.; Wang, S. *Polymer* **2003**, *44*, 1733−1739.
(39) Pittman, C. U., Jr.; Xu, X.; Wang, L.; Toghiani, H. *Polymer* **2000**, *41*, 5405−5413.
(40) Cao, X.; Zhang, L. *J. Polym. Sci., Part B: Polym. Phys.*, in press.
(41) Son, T. W.; Lee, D. W.; Lim, S. K. *Polym. J.* **1999**, *31*, 563−568.
(42) Bikiaris, D.; Prinos, J.; Botev, M.; Betchev, C.; Panayiotou, C. *J. Appl. Polym. Sci.* **2004**, *93*, 726−735.
(43) Martin, D.; Meijs, G. F.; Renwick, G. M.; Gunatillake, P. A.; McCarthy, S. J. *J. Appl. Polym. Sci.* **1996**, *60*, 557−571.
(44) Krause, S. *J. Macromol. Sci., Rev. Macromol. Chem.* **1972**, *7*, 251−273.

BM0495598